J Mater Sci (2016) 51:1522–1531
DOI 10.1007/s10853-015-9473-3

Unique performance of poly(*p*-phenylene terephthamide) hollow fiber membranes

Chun Wang[1] · Changfa Xiao[1] · Mingxing Chen[1] · Qinglin Huang[1] · Hailiang Liu[1] · Nana Li[1]

Received: 8 July 2015 / Accepted: 30 September 2015 / Published online: 13 October 2015

Abstract Poly(*p*-phenylene terephthamide) (PPTA) hollow fiber membrane with outstanding thermal and chemical stability (endures above 60 °C and almost any organic solvents) has been fabricated by dry–wet spinning method for the first time. The heat and solvent resistance as well as anti-fouling performances was studied in this paper. The properties of thermal stability were characterized by pure water flux, mechanical strength, FTIR, and pore size distribution, and the properties of chemical resistance were characterized by organic solvent flux. The results showed that PPTA hollow fiber membrane was a kind of inner and outer dual-skin layer structure. The flux was stable in hot water and organic solvents, which indicated that the membrane structure hardly changed. The average pore size was slightly increased during high-temperature experiment. Moreover, the properties of anti-fouling were characterized by simulated activated sludge filtration. The fouled PPTA membranes were cleaned by ultrasonic, citric acid, and alkali treatments, and the membrane surface was detected by energy-dispersive X-ray spectroscopy. The results showed that the effect of the citric acid treatment was more preferable to the other ways, which indicated that the inorganic substance was easily adsorbed on the membrane surface compared with organic substance. Therefore, PPTA hollow fiber membrane exhibited the excellent anti-fouling performance by the reason of strong hydrophilicity and electronegativity.

✉ Changfa Xiao
tjpuxiao@qq.com; xiaochangfa@163.com

[1] State Key Laboratory of Separation Membranes and Membrane Processes, School of Materials Science and Engineering, Tianjin Polytechnic University, Tianjin 300387, People's Republic of China

Introduction

Membrane separation technology is a new separation technology which uses membrane to complete the process of separation, purification, and concentration of the mixtures. Polymeric membranes have been widely used because of good workability, enormous varieties, and cheap price. However, there is a lack of stability of the most polymeric materials under extreme conditions, such as at high temperature, processes coupled to acid and alkali solution, or in the presence of organic solvents [1]. Nowadays, there is an increasing demand for heat- and solvent-resistant membranes for processes related to pharmaceutical, chemical synthesis, petrochemical, textile, and dyeing industries. But most of commercial polymeric membranes cannot be applied for these applications. Ceramic membranes still have undeniable advantages in these occasions, while they are worried about the high cost and difficult manufacture process, which restricts further application in the aspect of wastewater treatment [2]. Therefore, it is of great significance to develop the higher performance polymeric membrane.

Although polymeric membranes generally poorly maintain their physical integrity in extreme conditions because of their tendency to shrink or swell and even dissolve, it is possible to obtain ultrafiltration membranes for these areas [3]. It is reported that several membranes are suitable for high-temperature or organic solvents' operation in the literature. Wanbin Li et al. [4]. have prepared thermally stable and solvent-resistant self-cross-linked TiO_2/PAN hybrid hollow fiber membrane. B. Schulz et al. [5]. have prepared aromatic poly(1,3,4-oxadiazole)s as advanced materials. Chemical stability for organic solvent-resistant filtration is mainly attained by chemical cross-linking method to avoid shrinking or swelling.

Examples are integrally skinned asymmetric cross-linked polyimide (PI) nanofiltration membrane reported by I. Soroko et al. [6] and integrally skinned cross-linked asymmetric Matrimid®-based PI membranes with *p*-xylylenediamine reported by K. Vanherck et al. [7]. However, it is regretful that they have poor anti-wetting properties despite many useful properties, which accelerates fouling in the membrane separation process due to hydrophobicity.

PPTA is a kind of rigidly linear chain aromatic polyamide which has been widely used to prepare high-performance fibers because of its superior mechanical strength [8]. However, there is very little relevant research in the field of membranes. K. Nakura et al. [9]. have prepared ultrafiltration membranes using PPTA as a membrane material. Zschocke and Strathman [10] have reported a solvent-resistant membrane from PPTA. But the prepared PPTA flat membranes have a low permeation, which restricts their prospect of the application. Chun Wang et al. [11]. have published a kind of hybrid porous flat membrane from PPTA.

Although PPTA membranes are suitable for these extreme conditions due to the excellent thermal stability and great chemical stability and hydrophilicity, as is well known, these are especially difficult to produce owing to the non-melting and insoluble properties [12]. Not only do the strong hydrogen bonds interact among PPTA molecular chains, but also the decomposition temperature below its melting point prohibits the melt spinning method. Furthermore, the most common organic solvents cannot dissolve PPTA resin, while only the inorganic acid such as concentrated H_2SO_4 can overcome this difficulty.

In this article, a unique PPTA hollow fiber membrane has been fabricated by dry–wet spinning method. PPTA resin is used as the polymeric material, H_2SO_4 as the solvent, SiO_2 as the additive, and the mixture of polyethylene glycol (PEG) and polyvinylpyrrolidone (PVP) as the pore formation agent. This article aims to investigate the heat and organic solvent resistance of PPTA hollow fiber membrane and observe the anti-fouling performance. The unique properties of PPTA hollow fiber membrane will allow the application for these harsh operation conditions which have been hardly possible for polymeric materials, opening perspective to compete with ceramic membranes in a much broader range of applications.

Experimental materials and methods

Materials

Poly(*p*-phenylene terephthamide) resin (PPTA, fiber grade, $\eta_{inh} = 5.5–6.5$ dL/g) was purchased from Suzhou Zhaoda Specially Fiber Technical Co. Ltd. Concentrated sulfuric acid (H_2SO_4, 98 %, AR) was purchased from Tianjin Fengchuan Chemical Reagent Technologies Co. Ltd. Fuming sulfuric acid ($H_2SO_4{\cdot}XSO_3$, $SO_3 \approx 20$ wt.%) was purchased from Shanghai Zhenxing No. 2 Chemical Plant Co. Ltd. Silica (SiO_2) particles with an average size of 30 nm were purchased from Beijing Boyu Gaoke Advanced Materials Technical Co. Ltd. Polyethylene glycol (PEG, $M_w = 2000$, AR) and polyvinylpyrrolidone (PVP, $M_w = 30{,}000$, AR) were purchased from Tianjin Kemel Reagent Co. Ltd. The commercial PVDF hollow fiber membranes (OD/ID: 1.2 mm/0.7 mm; pore size: 0.03 μm) were provided by Tianjin Motimo Membrane Technology Co. Ltd. *N*,*N*-Dimethylacetamide (DMAC, AR), trichloromethane ($CHCl_3$, AR), tetrahydrofuran (THF, AR), and *N*-methyl-2-pyrrolidone (NMP, AR) were purchased from Tianjin Guangfu Fine Chemical Institute.

Membrane preparation

First of all, PPTA resin and SiO_2 particles were dried for 12 h at 100 °C in a vacuum oven (0.1 MPa) to remove moisture. Then, at 80 °C they were in a special weight homogeneously mixed with H_2SO_4 and pore-forming agents in sealed stirring tank under high-speed agitation. Subsequently, the completely dissolved casting solution was degassed by a vacuum pump (0.1 MPa). The spinning dope was extruded through a spinneret, and the nascent polymeric fiber membranes first passed through an air-gap region and then entered the distilled water external coagulation bath. Finally, PPTA hollow fiber membranes were fabricated by the dry–wet spinning process. After that, the as-spun hollow fiber membranes were immersed in tap water for 48 h to remove residual solvent.

Characterization of membrane

Scanning electron microscopy (SEM)

The surface and cross-section morphology of membranes was observed by field emission scanning electron microscopy (FESEM, Nano-230, FEI, Czech). The membranes were freeze dried before cryogenically fractured in liquid N_2, and they were sputtered with gold.

Permeation and separation

Membrane permeation was characterized by pure water flux (PWF) under different temperature tests. The pressure difference across the membrane was 0.1 MPa. The PWF was determined by Eq. (1):

$$J = \frac{V}{A \times t}, \quad (1)$$

where J is the PWF (L $m^{-2}h^{-1}$), V is the total quantity of permeation (L), A is the membrane area (m^2), and t is the testing time (h).

In this paper, BSA solution was also chosen to perform the thermal rejection. The membrane module contained four hollow fiber membranes with an effective length of 15 cm. All the experiments were tested at 25 and 60 °C, respectively. Before the test, each membrane was initially compacted for 10 min at 0.15 MPa, and then the flux was recorded at 0.1 MPa every 5 min until the completion at 30 min. The BSA (1 g/L) solution was prepared in distilled water. The rejection rate was calculated by Eq. (2) [13]:

$$R = \left(1 - \frac{C_p}{C_f}\right) \times 100\,\%, \tag{2}$$

where C_p and C_f are the permeate and feed density, respectively. The absorbance of feed and filtration solutions was determined by UV spectroscopy at 280 nm, using a Beijing Purkinje UV-1810 spectrophotometer.

Pore size distribution

Pore size distribution was characterized by mercury intrusion porosimeter (Auto pore iv-9500). The samples should be totally dried out prior to testing.

Mechanical properties

Mechanical properties were measured by Electronic Stretching Machine (CMT-4204, MTS systems, Co. Ltd) at room temperature. The tensile rate was 100 mm min^{-1} and the gripping length was 50 mm. The PPTA membrane's parameters of OD/ID were about 2.1 mm/1.3 mm, and the PVDF membrane's parameters of OD/ID were about 1.2 mm/0.7 mm. The average value of five tests was chosen (Table 1).

Table 1 The parameters of PPTA hollow fiber membranes

	Sample parameter
Dope composition (wt.%)	(2.0 % PPTA)/H_2SO_4
Additive (wt.%)	0.5 % SiO_2
Bore fluid	Distilled water
Bore fluid speed (ml/min)	20
Extra coagulation	Tap water
Extra coagulation (T/°C)	20
Air gap(mm)	15
Take-up speed (m/min)	15
Spinneret dimension (mm)	OD/ID 2.0/1.2

Fourier transform infrared spectrum (FTIR)

IR spectra of the samples were recorded by a Bruck Tensor 37 IR spectrophotometer in a wavenumber range from 400 to 4000 cm^{-1}. The spectral resolution was 4 cm^{-1}. The samples for IR analysis were prepared at 25 °C in the form of KBr pellets.

Simulated activated sludge filtration

In order to further evaluate the fouling resistance properties, simulated activated sludge process was introduced to characterize the PPTA hollow fiber membrane. The schematic diagram of simulated activated sludge process is shown in Fig. 1. During 3 months, the sludge solution was continuously filtered to produce ultrafiltration water under the constant self-priming pump pressure, and the cross-flow filtration was used in this experiment. Besides, there were ten membrane modules, each of which contained three PPTA hollow fiber membranes with an effective length of 15 cm. In this study, the activated sludge was obtained from the real membrane bioreactor (MBR) system, and the particle size distribution was researched with laser particle size analyzer (HORIBA LA-300, Japan). The concentration of mixed liquor suspended solids (MLSS) was approximately 10,000 mg/L (as shown in Fig. 2). The potassium dichromate titration method was a regular method to determine chemical oxygen demand (COD) and COD removal rate (CRR %), which demonstrated the removal rate of organic pollutants.

After the fouling experiment, the membranes were introduced to three kinds of membrane chemical cleaning plus backwash treatments: the first method was to clean by ultrasonic oscillation in an hour; the second method was to immerse in 1.0 wt.% NaOH solution for 3 h; and the third method was to immerse in 1.0 wt.% citric acid solution for 3 h. Finally, all above membranes were repeatedly flushed

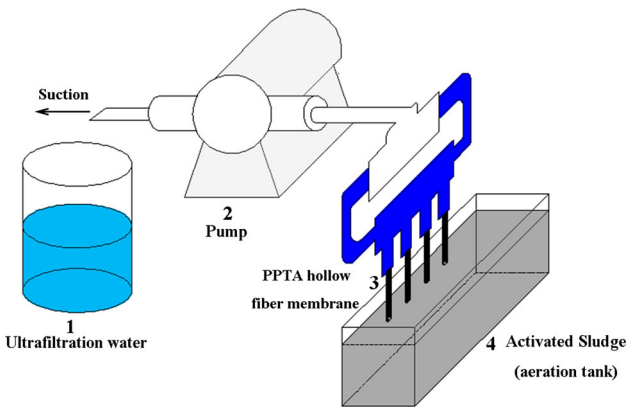

Fig. 1 The schematic diagram of simulated activated sludge process

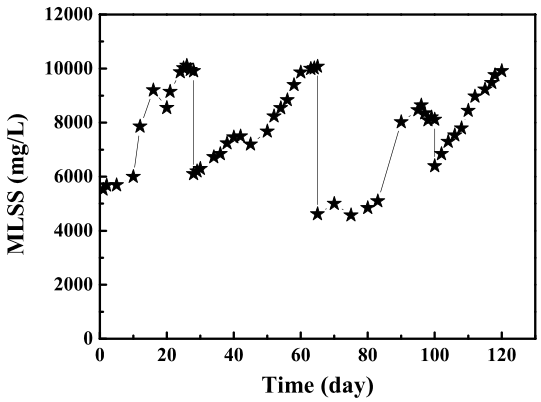

Fig. 2 Variation of MLSS in simulated activated sludge process

by water three times, and every times lasted 10 min. Then, the morphology and energy-dispersive X-ray spectroscopy (EDX) data of outer surface elements were observed by FESEM (S-4700, Hitachi, Japan).

In order to evaluate the clean effects by different backwash methods, the flux recovery ratio (FRR) was calculated using Eq. (3) [14]:

$$\mathrm{FRR} = \left(\frac{Jw_1}{Jw_2}\right) \times 100\,\%, \tag{3}$$

where Jw_1 is the PWF (L $m^{-2}h^{-1}$) of the cleaned membranes and Jw_2 is the PWF (L $m^{-2}h^{-1}$) of the uncontaminated membranes.

Results and discussion

Morphology of membrane

The FESEM photographs in Fig. 3 show the morphology of PPTA hollow fiber membrane and the effect of thermal separation on the morphology. Figure 3a and b shows the morphology of the outer and inner surfaces, respectively, and Fig. 3c and d shows the morphology of cross section; then Fig. 3e and f shows the morphology of cross section after pure water filtration at 90 °C.

Figure 3a and b indicates some differences in morphology between the inner and outer surfaces of PPTA hollow fiber membrane. The outer surface is denser than the inner one; however, no obvious micro-pores can be identified on the inner surface. It is a kind of dual-skin layer structure other than the asymmetrical structure of PPTA flat membrane [15]. The polymeric spinning solution immerses into non-solvent coagulant bath and the bore fluid forms hollow structure, then they turn up instantaneous liquid–liquid phase inversion. When the polymeric spinning solution extruded from the spinneret, the outer surface first solidifies owing to exposure to cool air gap and then immerses into coagulant bath, while the inner surface solidifies relatively slowly [15]. Therefore, although the diffusion rates are slightly different, the same outer and inner non-solvent coagulant solution forms the dual skin layer.

Figure 3c and d shows that the cross section of PPTA hollow fiber membrane is a kind of well-distributed finger-like macro-void structure. After thorough 24-h hot water filtration, Fig. 3c–f shows few significant differences in the morphology of the cross section, which indicates that there is hardly a change in the membrane structure.

Permeation and mechanical properties

Figure 4 shows the effect on permeability at high temperature. The thermal flux of PPTA and commercial PVDF hollow fiber membranes is shown in Fig. 4a, and 60 and 90 °C are selected as the test temperature. In this study, two kinds of samples are continuously tested for 24 h, and the thermal flux reaches nearly stable value in 4 h; then the results of 7 h are chosen to exhibit the heat resistance of membrane. As shown in Fig. 4a, it is obvious that the commercial PVDF hollow fiber membrane has higher PWF, while there is also another disadvantage that the flux decay rate can reach 40–50 %. Meanwhile, PPTA is a rigidly linear chain macro-molecule and decomposes above 450 °C, which can prevent the pore structure from undergoing deformation and then maintain stable flux under thermal condition. Thus, it should be noted that this is a great advantage for the high-temperature membrane separation process.

Moreover, Fig. 4b shows the thermal organic solvent flux of PPTA hollow fiber membrane, and in Fig. 4c, the PPTA hollow fiber membranes prepared in this work are tested regarding its stability in different organic solvents. As shown in Fig. 4b and c, DMAC, NMP, $CHCl_3$, and THF are chosen as several typical organic solvents. The result indicates that no mass loss is observed after thermal filtration, and PPTA membrane can undergo very little shrinking and swelling effects in organic solvents, which is found to be a significant role in this study.

Figure 5 shows the effect of high temperature on mechanical properties. As shown in Fig. 5a, three curves of PPTA membrane exhibit a very linear relationship, tensile strength–strain decreases with rising temperature. It will quickly drop to zero when tensile strength reaches breaking point. On the contrary, the curves of PVDF membrane conform to typical tensile strength–strain of flexible polymer [16, 17]. When the temperature is 25 °C, the curve of PVDF-25 membrane appears stress yield area other than PPTA-25 membrane. As for membrane materials, it is significant that the micro-pore structure remains stable as much as possible, which ensures the smaller decline of

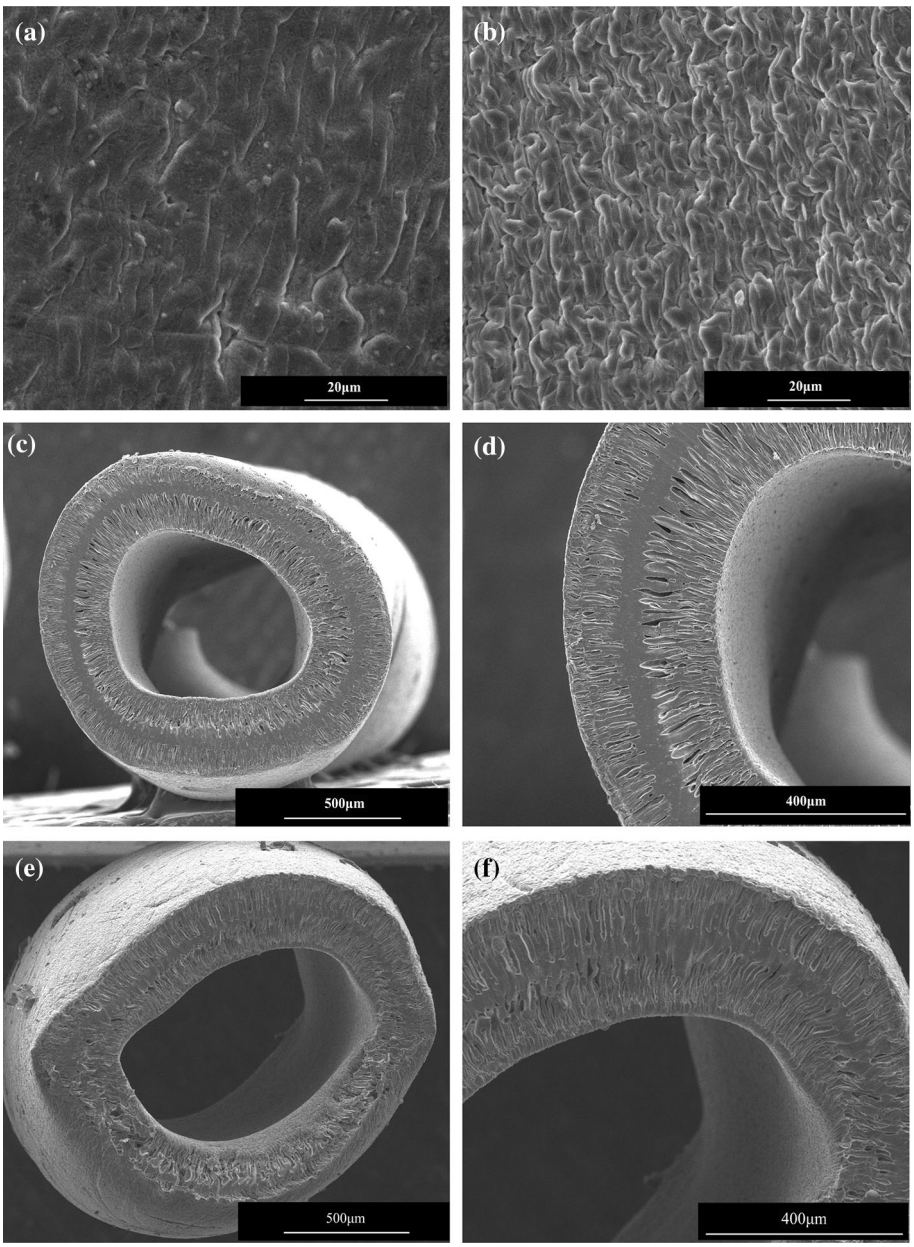

Fig. 3 The morphologies of PPTA hollow fiber membrane. **a** Outer surface, **b** inner surface, **c** and **e** cross section, and **d** and **f** partially enlarged drawing

membrane performances in a long period of time. As shown in Fig. 5, PPTA membrane shows a much lower strain to break compared to PVDF at high temperature because of the PPTA rigid chain polymer. Combined with the above Fig. 4a, the PPTA curves of thermal flux exhibit a linear relationship at high temperatures. Therefore, the PPTA membrane structure can possess sufficient pore support stability to withstand the exchange of different temperatures.

Mercury intrusion porosimeter is used to characterize the change of pore distribution during thermal filtration process. Figure 6 shows the effect of high temperature on pore size distribution. As shown in Fig. 6, there is little difference between 25 and 90 °C. Before and after experiment, it is easy to possess small pores and a narrow pore size distribution. The mean pore size of PPTA-25 is almost 13.9 nm, while that of PPTA-90 is 16.2 nm. This is due to a high degree of crystallinity of PPTA macro-molecule [18], and the temperature of pore deformation is higher. Thus the result is consistent with the cross-section morphology of Fig. 3, which exhibits excellent thermal stability.

FTIR

To confirm whether the hydrogen bonds have changed before and after thermal experiments, they are investigated by a transmission FTIR spectrophotometer. Fig. 7 shows the comparison of the FTIR spectra of PPTA membranes at

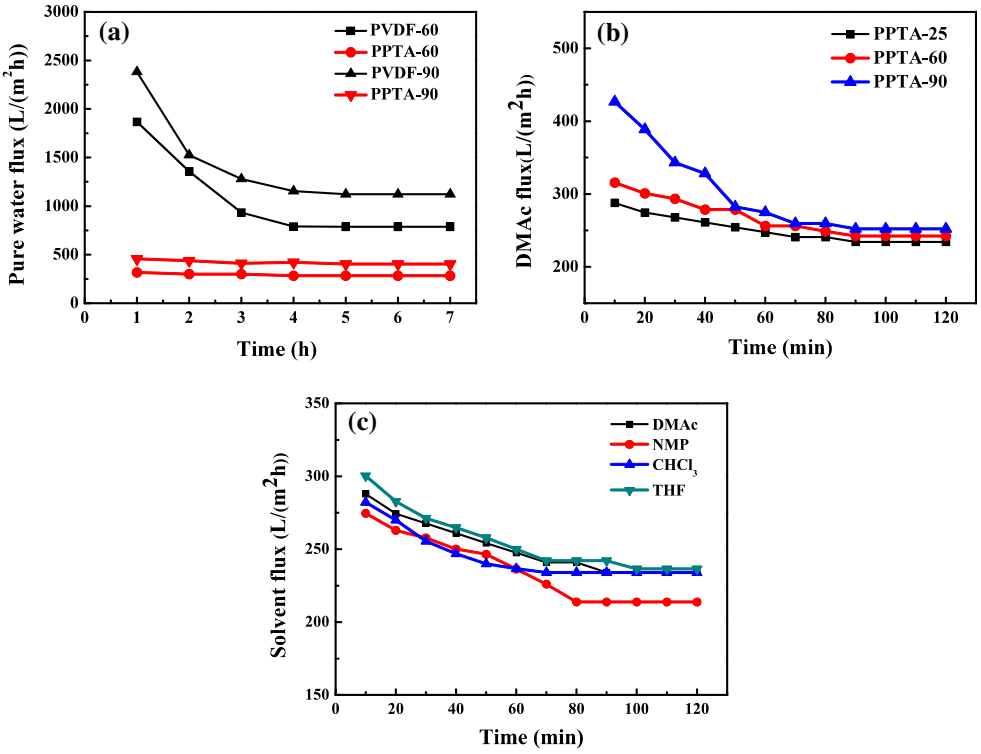

Fig. 4 Effect on permeability under high temperature and organic solvents. **a** Pure water flux, **b** DMAC thermal flux, and **c** organic solvent flux

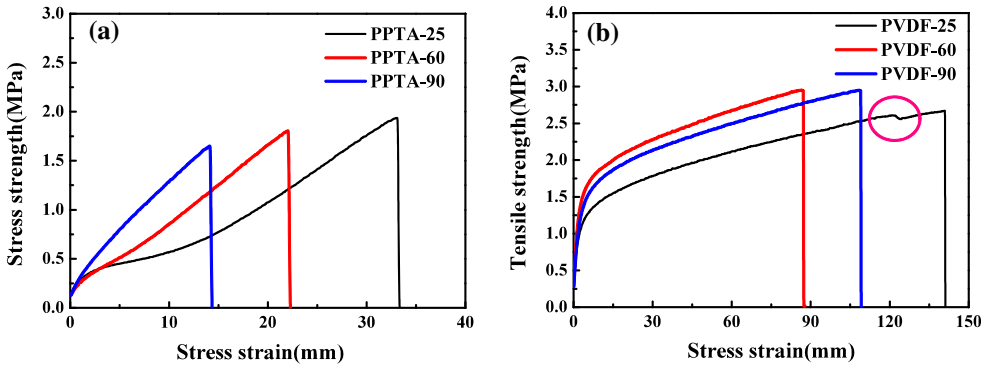

Fig. 5 Effect on mechanical properties at high temperature

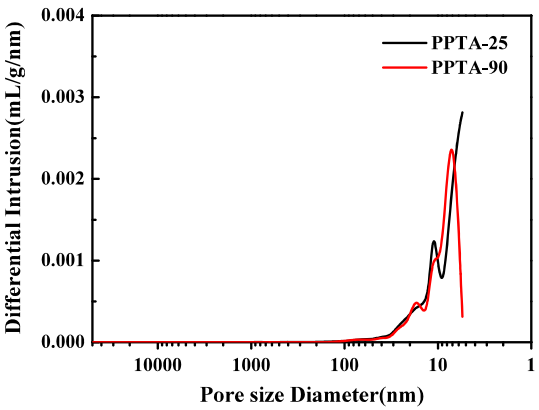

Fig. 6 Pore size distribution of PPTA hollow fiber membrane at different temperatures

25 and 90 °C. As is known to all, not only aramid polymer has rigid aromatic rings, the organizational structure built by the hydrogen bonds also has a significant impact on its performance [19]. The results show that there is no difference in chemical structure with the two samples. However, there is a tiny difference in the intensity of groups in the peak wave transmittance. The two bands near 3300–4000 cm^{-1} are assigned to O–H and N–H stretching vibration, and 1200–1600 cm^{-1} band is assigned to C–N wagging-bending vibration. The three bands of PPTA-90 are slightly greater than PPTA-25. This is due to the greater association degree of hydrogen bond, and N–H absorption peak is moving toward the direction of low wave number. Therefore, the movement of molecular chain is limited because of the increase of hydrogen bond density, which

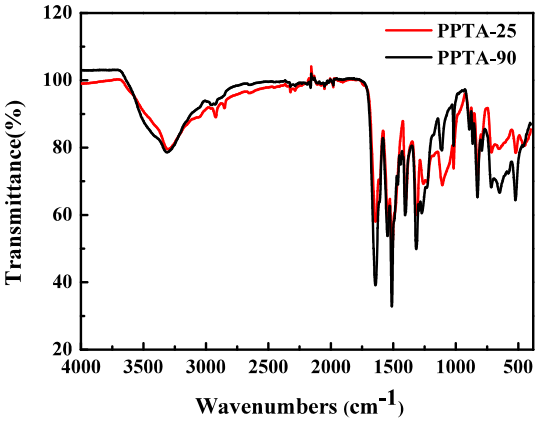

Fig. 7 FTIR spectra of PPTA hollow fiber membranes

generates the more stable pore structure, and then the water flux is still stable at high temperature and the pore size distribution becomes narrower.

Rejection

As is known to all, rejection properties can effectively reflect the membrane separation performance. Thus we will focus on the effect on thermal rejection in this study. Although protein molecules are easy to inactivate under thermal circumstances, the experimental results of thermal separation have still referential significance in this paper. BSA solution (1 g/L) is chosen to perform the thermal rejection. Figure 9 shows the rejection rate of PPTA and commercial PVDF hollow fiber membranes at 25 and 60 °C. It is obvious that both of them can reach more than 90 % at low temperature condition; however, the PPTA membrane still remains at 90 % while the PVDF only reaches 20 % at high temperature. Moreover, Fig. 8 shows the morphology of inner surface of PPTA and commercial PVDF hollow fiber membranes. As shown in Fig. 8b, the inner surface of PVDF membrane undergoes serious cracking phenomenon, which can be the main reason for the lower rejection rate.

Anti-fouling performance

To determine the flux behavior during cross-flow filtration, which is determined as the effect on fouling resistance, the filtration recycle experiments are characterized by the BSA ultrafiltration. The results are shown in Fig. 10. The ultrafiltration process can be divided into three parts: The first 1 h in the curve is referred to as pure water ultrafiltration. Then the second half an hour is BSA solution ultrafiltration. Finally, the third is the membrane backwash which is flushed by pure water, and then recycle the three processes. As shown in Fig. 10, in the case of BSA solution, the protein molecules attach quickly on the membrane surface within first 15 min of exposure and membrane fouling begins, the flux obviously decreases and then gradually reaches stable value. This is caused by concentration polarization [20]. The protein molecules may pile on the membrane surface and block the pore channels. After recycling for three times, it is observed that irreversible membrane fouling is not severe during BSA solution ultrafiltration after backwash, and the flux shows a nearly complete recovery. It is indicated that the PPTA membrane maintains higher steady-state flux due to great hydrophilicity [21].

This study also importantly focuses on the great anti-fouling properties. FESEM images of cleaned and fouled PPTA membrane are presented in Fig. 11. The surface properties play an important role in determining the fouling resistance properties of membranes. It obviously reveals that the fouled membranes are covered with gel layer in Fig. 11e1, e2. As the gel layer is developed, it will be difficult to remove the layer from the membrane surface.

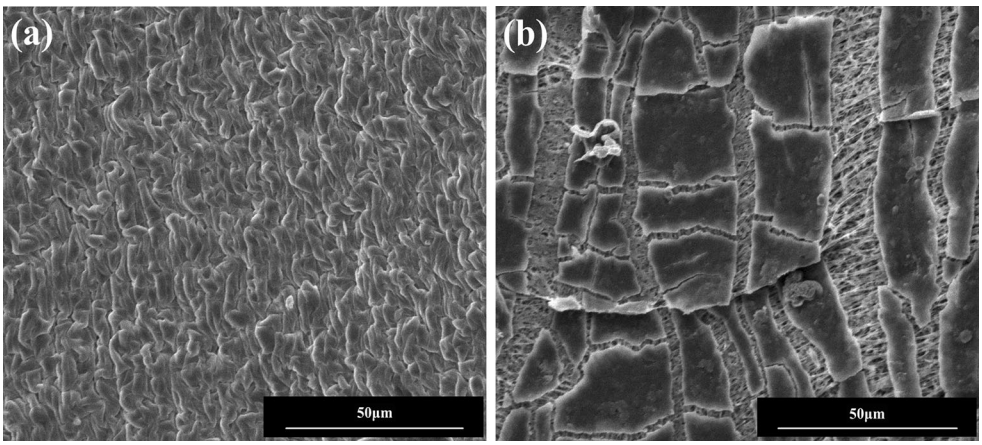

Fig. 8 The morphologies of inner surface of PPTA and commercial PVDF hollow fiber membranes via thermal rejection process. **a** PPTA and **b** PVDF

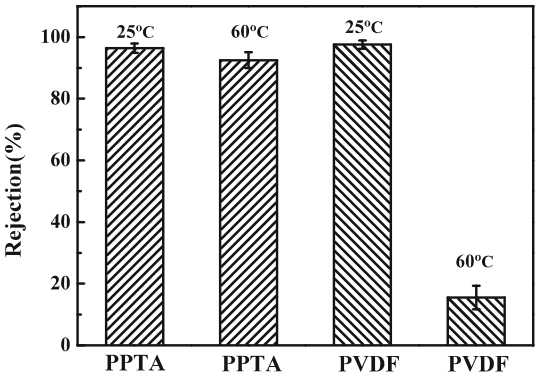

Fig. 9 The rejection of PPTA and commercial PVDF hollow fiber membranes at different temperatures

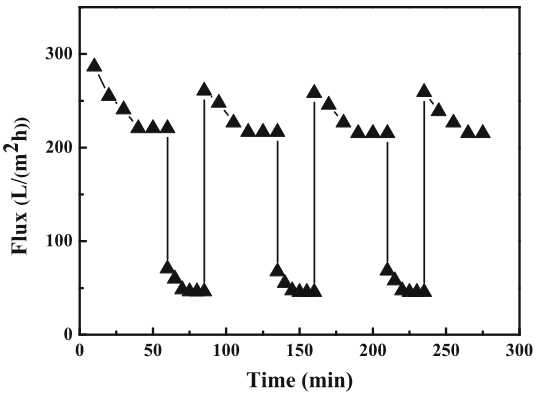

Fig. 10 Flux behavior during cross-flow filtration of the PPTA hollow fiber membrane with three recycles of BSA solution (1 g/L)

Thus, for the purpose of the recovery of performances, the effective wash methods are taken into consideration to remove the gel layer [22, 23]. Membrane fouling can be categorized into bio-fouling, organic particle fouling, and inorganic particle fouling, and the cleaning methods are divided into physical and chemical methods. In general, inorganic pollutants are usually cleaned by acid solution such as hydrochloric acid (HCl), citric acid, or oxalic acid. Meanwhile, organic pollutants are cleaned by alkali solution or oxidizing agents such as sodium hypochlorite (NaClO) and hydrogen peroxide (H_2O_2). Specially speaking, NaClO is very commonly used for cleaning the membranes affected by organic particle fouling; however, PPTA has poor chlorine and oxidation resistance, which results in easy decomposition under this situation. Therefore, in this paper, it is accepted that ultrasonic treatment as physical cleaning is used as well as NaOH and citric acid as chemical cleaning. As shown in Fig. 11d1, d2, the backwash effect of citric acid is apparently superior to the other two ways. What is more, the COD removal rate of membrane modules can reach more than 99 %, and the FRR of PPTA membrane by citric acid nearly reaches 90 % (as shown in Fig. 13).

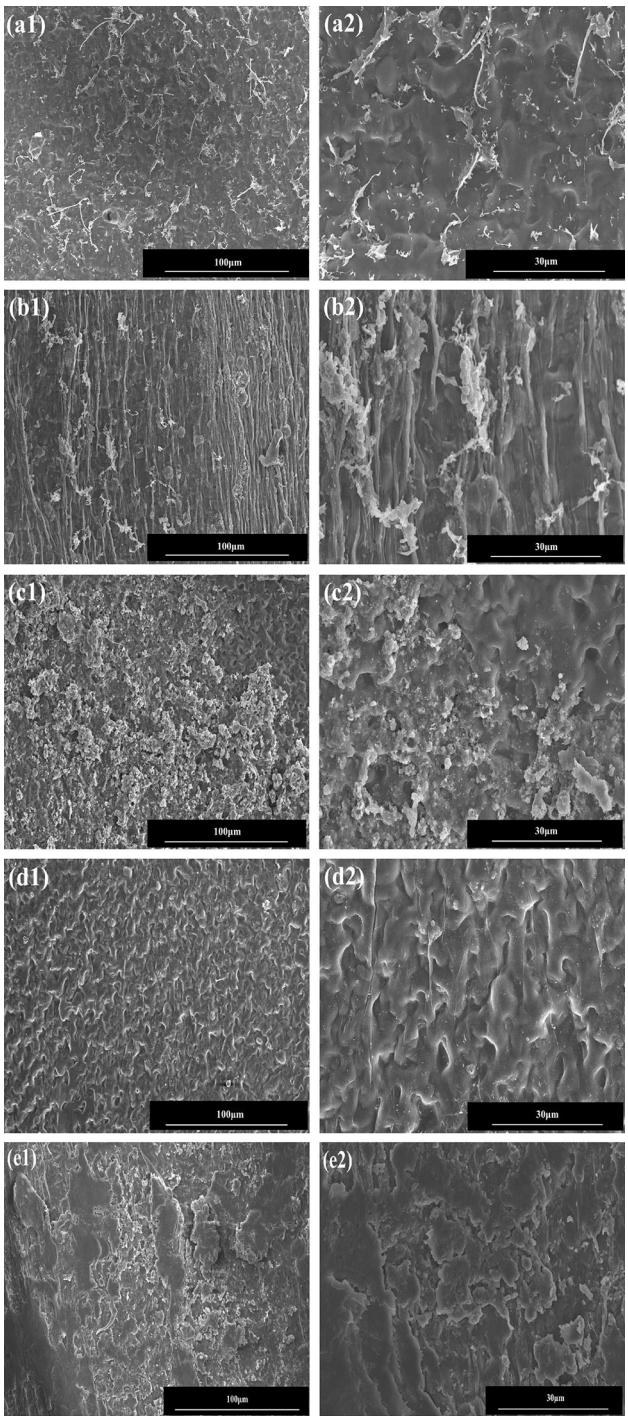

Fig. 11 The outer surface morphologies of PPTA hollow fiber membranes by different treatments. **a** Surface adsorption, **b** ultrasonic, **c** NaOH, **d** citric acid, and **e** sludge pollution, **1** polluted surface, **2** backwash surface

Element analysis is further performed on the surface layer in order to identify the chemical components of the layer by EDX. The main elements of C, O, S, Si, Na, K, Ca, Mg, Al, and Cl are detected (as shown in Fig. 12). Combined with the above-mentioned morphology in Fig. 11,

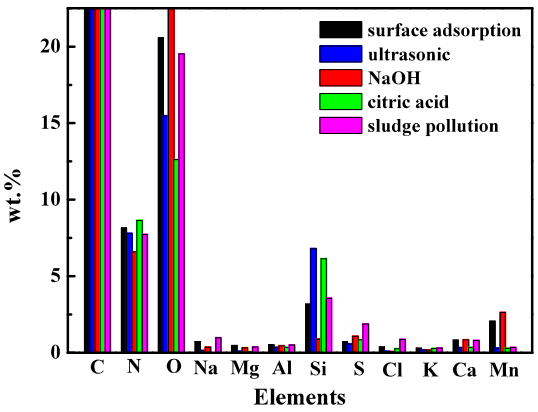

Fig. 12 The element analysis of PPTA hollow fiber membranes by EDX

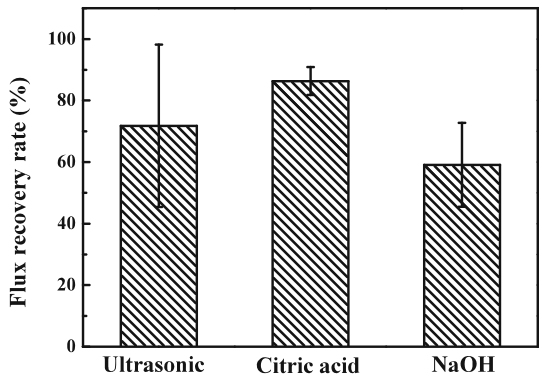

Fig. 13 The FRR of PPTA hollow fiber membrane by three backwash treatments

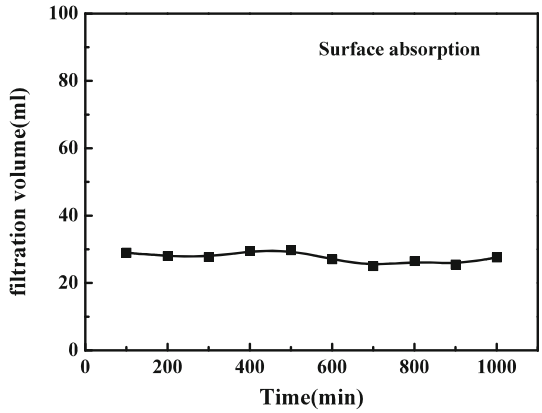

Fig. 14 The pure water filtration of PPTA hollow fiber membrane by surface absorption

Na^+, Mg^{2+}, Al^{3+}, Si^{4+}, K^+, and Ca^{2+} have significant effects on the formation of gel layer [24, 25].

According to the analysis of EDX images in Fig. 12, ultrasonic method has some influence on the removal of extracellular polymer substances (EPS). However, an amount of adherent gel groups still deposits on the membrane surface. What is worse, the membrane structure subjects to damage , that is, the element of Si appears as a sharp peak, which suggests that it is possible that SiO_2 inorganic particles embedded inside the membrane are revealed on the membrane surface. Alkaline compounds are used to clean organic pollutants or microbial substance. However, compared with the EDX spectrum of sludge pollution, there are hardly significant differences among the absorption peaks such as the elements of K^+, Al^{3+}, and Ca^{2+}. Then, citric acid can effectively dissolve and remove mineral salts or metal oxide, which will trigger complexation reactions among them, so that the inorganic pollutants are stripped away from the membrane surface [26, 27]. As a result, PPTA membrane has great resistance to organic pollutant, meanwhile the inorganic pollutant is the main factor for PPTA membrane fouling (Fig. 13).

Moreover, as for PPTA membrane, it is an interesting exploration that the main source of pollution is caused by surface adsorption or pollution sediment. Thus the another PPTA hollow fiber membranes are immersed in simulated activated sludge tank at the same time, and then the PWF is tested again until it reaches stability every time. It is worth noting that the curve of PWF exhibits a very linear relationship in Fig. 14, which demonstrates that the pollutants hardly absorb on the membrane surface, they are easily flushed away under cross-flow condition, and they do not form embedded pollution. At present, it is widely accepted that the more hydrophilic the membrane surface, the better the anti-fouling performance. The contact angles may reach 20°–40° of PPTA membrane in accordance with previous studies by Chun Wang et al. [11]. The reason is that, on the one hand, the hydrophilic surface is favorable to combine with water molecules, aiming to form hydrogen bonds; on the other hand, the N–H bonds of PPTA molecules have strong electronegativity. Therefore, pollution sediment is proved to be the main factor again.

Conclusion

PPTA hollow fiber membrane has been prepared via dry–wet spinning method for the first time. The obtained membrane is a kind of dual-skin layer structure, and the cross section is a kind of well-distributed finger-like macro-void. Under high temperature circumstances, the mean pore size is measured to be about 16 nm and the thermal water flux fails to decline for time dependence, which indicates that PPTA membrane has great heat resistance performance. Then, the PPTA membranes are able to stably operate in organic solvent, and the shrinking or swelling effects are found to be insignificant, so the PPTA membrane proves to be stable in solvent tested.

What is more, the anti-fouling performances of PPTA membranes are already taken into consideration in this study. The COD removal rate of membrane modules can reach more than 99 %. Then three different kinds of backwash treatments are adopted to treat the polluted PPTA membranes, and consequently as it is clearly seen from the FESEM images and EDX, the backwash effect as well as FRR in case of citric acid treatment is apparently superior to other two ways. PPTA hollow fiber membranes especially exhibit difficult surface adsorption property owing to strong hydrophilicity and electronegativity.

Acknowledgements The authors gratefully acknowledge the financial support of the National Basic Research Program of China (2012CB722706), the National Natural Science Foundation of China (21274109), the Science and Technology Plans of Tianjin (13JCQNJC02100), and the Specialized Research Fund for the Doctoral Program of Higher Education (20131201120003).

References

1. Pendergast MM, Hoek EMV (2011) A review of water treatment membrane nanotechnologies. Energy Environ Sci 4(6):1946–1971. doi:10.1039/C0EE00541J
2. Maab H, Pereira Nunes S (2013) Porous polyoxadiazole membranes for harsh environment. J Membr Sci 445:127–134. doi:10.1016/j.memsci.2013.05.038
3. Shukla JS, Dixit SK (1992) Synthesis of some new wholly aromatic heat resistant polyhydrazides as possible polymers for membranes (desalination). Eur Polym J 28(2):199–202. doi:10.1016/0014-3057(92)90308-O
4. Li W, Yang Z, Meng Q, Shen C, Zhang G (2014) Thermally stable and solvent resistant self-crosslinked TiO_2/PAN hybrid hollow fiber membrane fabricated by mutual supporting method. J Membr Sci 467:253–261. doi:10.1016/j.memsci.2014.05.019
5. Schulz B, Bruma M, Brehmer L (1997) Aromatic poly(1, 3, 4-oxadiazoe)s as advanced materials. Adv Mater 9(8):601–613. doi:10.1002/adma.19970090804
6. Soroko I, Lopes MP, Livingston A (2011) The effect of membrane formation parameters on performance of polyimide membranes for organic solvent nanofiltration (OSN): part A. Effect of polymer/solvent/non-solvent system choice. J Membr Sci 381(1–2):152–162. doi:10.1016/j.memsci.2011.07.027
7. Vanherck K, Vandezande P, Aldea SO, Vankelecom IFJ (2008) Cross-linked polyimide membranes for solvent resistant nanofiltration in aprotic solvents. J Membr Sci 320(1–2):468–476. doi:10.1016/j.memsci.2008.04.026
8. Li SFY, McGhie AJ, Tangt SL (1993) Internal structure of Kevlar fibres by atomic force microscopy. Polymer 34:4573–4575
9. Nakura K, Kamizawa C, Matsuda M, Masuda H (1992) Preparation of ultrafiltration membranes using poly(*p*-phenyleneterephthalamide) as a membrane material. Maku 17(2):78–84
10. Zschocke P, Strathmann H (1980) Solvent resistant membranes from poly-(*p*-phenylene-terephthalamide). Desalination 34(1–2):69–75. doi:10.1016/S0011-9164(00)88581-1
11. Wang C, Xiao C, Huang Q, Pan J (2015) A study on structure and properties of poly(*p*-phenylene terephthamide) hybrid porous membranes. J Membr Sci 474:132–139. doi:10.1016/j.memsci.2014.09.055
12. Denchev Z, Dencheva N (2012) Manufacturing and properties of aramid reinforced composites. Hanser, Munich, pp 251–280. doi:10.3139/9781569905258.008
13. Chen W, Su Y, Zhang L, Shi Q, Peng J, Jiang Z (2010) In situ generated silica nanoparticles as pore-forming agent for enhanced permeability of cellulose acetate membranes. J Membr Sci 348(1–2):75–83. doi:10.1016/j.memsci.2009.10.042
14. Zhang X, Xiao C, Hu X, Jin X, Bai Q (2013) Study on the interfacial bonding state and fouling phenomena of polyvinylidene fluoride matrix-reinforced hollow fiber membranes during microfiltration. Desalination 330:49–60. doi:10.1016/j.desal.2013.09.022
15. Boom RM, Wienk IM, van den Boomgaard T, Smolders CA (1992) Microstructures in phase inversion membranes. Part 2. The role of a polymeric additive. J Membr Sci 73(2–3):277–292. doi:10.1016/0376-7388(92)80135-7
16. Denchev Z, Dencheva N (2012) Preparation, mechanical properties and structural characterization of microfibrillar composites based on polyethylene/polyamide blends. Carl Hanser Verlag GmbH & Co, Munich, pp 465–524. doi:10.3139/9781569905258.014
17. Shi F, Ma Y, Ma J, Wang P, Sun W (2013) Preparation and characterization of PVDF/TiO_2 hybrid membranes with ionic liquid modified nano-TiO_2 particles. J Membr Sci 427:259–269. doi:10.1016/j.memsci.2012.10.007
18. Castro-Muñiz A, Martínez-Alonso A, Tascón JMD (2008) Modification of the pyrolysis/carbonization of PPTA polymer by intermediate isothermal treatments. Carbon 46(7):985–993. doi:10.1016/j.carbon.2008.02.004
19. Martínez-Felipe A, Imrie CT, Ribes-Greus A (2013) Study of structure formation in side-chain liquid crystal copolymers by variable temperature fourier transform infrared spectroscopy. Ind Eng Chem Res 52(26):8714–8721. doi:10.1021/ie303130e
20. Sui Y, Wang Z, Gao X, Gao C (2012) Antifouling PVDF ultrafiltration membranes incorporating PVDF-g-PHEMA additive via atom transfer radical graft polymerizations. J Membr Sci 413–414:38–47. doi:10.1016/j.memsci.2012.03.055
21. Hyun J, Jang H, Kim K, Na K, Tak T (2006) Restriction of biofouling in membrane filtration using a brush-like polymer containing oligoethylene glycol side chains. J Membr Sci 282(1–2):52–59. doi:10.1016/j.memsci.2006.05.008
22. Wang Z, Ma J, Tang CY, Kimura K, Wang Q, Han X (2014) Membrane cleaning in membrane bioreactors: a review. J Membr Sci 468:276–307. doi:10.1016/j.memsci.2014.05.060
23. Teli SB, Molina S, Sotto A, Calvo EG, Abajob Jd (2013) Fouling resistant polysulfone–PANI/TiO_2 ultrafiltration nanocomposite membranes. Ind Eng Chem Res 52(27):9470–9479. doi:10.1021/ie401037n
24. Wang Z, Wu Z, Yin X, Tian L (2008) Membrane fouling in a submerged membrane bioreactor (MBR) under sub-critical flux operation: membrane foulant and gel layer characterization. J Membr Sci 325(1):238–244. doi:10.1016/j.memsci.2008.07.035
25. Singh AK, Singh P, Mishra S, Shahi VK (2012) Anti-biofouling organic-inorganic hybrid membrane for water treatment. J Mater Chem 22(5):1834–1844. doi:10.1039/C1JM14250J
26. Lim AL, Bai R (2003) Membrane fouling and cleaning in microfiltration of activated sludge wastewater. J Membr Sci 216(1–2):279–290. doi:10.1016/S0376-7388(03)00083-8
27. Banerjee I, Pangule RC, Kane RS (2011) Antifouling coatings: recent developments in the design of surfaces that prevent fouling by proteins, bacteria, and marine organisms. Adv Mater 23(6):690–718. doi:10.1002/adma.201001215